

Numerical Solutions to Blunt Body Re-entry Problem

University of Notre Dame
Department of Aerospace and Mechanical Engineering

Prepared by: Jeffery D. Bruns

Prepared for: AME 48491 - Undergraduate Research,
Aleksandar Jemcov and Joseph M. Powers

Notre Dame, Indiana 46556

Date: July 8, 2014

Abstract

This report describes how using the Navier-Stokes equations to numerically calculate a shock wave will more accurately depict a realistic and observed shock wave. Earlier related inviscid shock capturing studies that have attempted to numerically calculate the shock wave and downstream field surrounding a blunt body re-entering the atmosphere have exhibited an instability known as the carbuncle phenomenon, which is not observed in nature. The use of high order shock-capturing methods has induced this instability in which the shock wave exhibits non-physical behavior. This study provides a new approach at calculating a numerical solution of the blunt body re-entry problem. Instead of using the Euler equations, the Navier-Stokes equations will be used, thus including physical damping in the problem. With the Navier-Stokes equations, the physical properties of the flow around the blunt body will be preserved in the numerical solution providing a solution in greater harmony with that seen in nature. In order to obtain this solution, the spatial and temporal resolution must be sufficiently fine to capture the shock. Since the shock wave is so thin, in the nanometer scale, the grid size in the domain surrounding the blunt body must be sufficiently small to capture the shock and not have the solution become unstable. The numerical solutions were calculated using OpenFOAM, a free, open source software system where the blunt body was a cylinder of radius 0.1 mm so that the computations are manageable.

1 Introduction

This report will describe how behavior of flow around a blunt body re-entering the atmosphere was predicted through numerical methods. An image of a blunt body under re-entry conditions is shown in Figure 1, which has a shock wave, boundary layer (not readily visible), and wake physically present during re-entry [1]. Many real engineering devices require

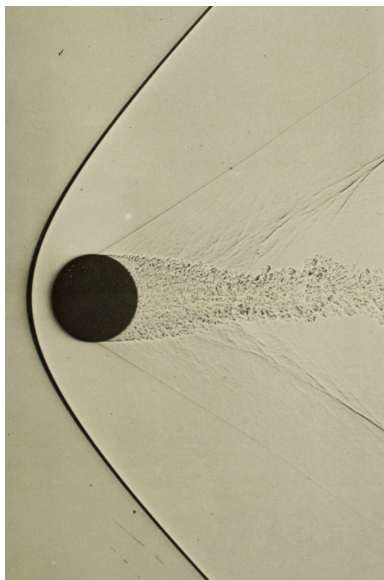


Figure 1: Shadowgraph image of sphere at $M = 1.53$, where a shock wave, boundary layer, and wake are present in the flow; figure from [1].

this information in order to better their performance, such as the Galileo Probe shown in Figure 2 [2]. The Galileo Probe was an atmospheric probe used to gather data from the planet Jupiter and return this information to Earth after re-entering the Jovian atmosphere. This device entered Jupiter's atmosphere without braking beforehand, and had to undergo extreme heating and pressurization. The probe was decelerated from 47.5 km/s to less than 1 km/s within the first hundred seconds of re-entry, and withstood a peak stagnation-point heating rate of 30 kW/cm² as it entered Jupiter's atmosphere to gather data [3]. It is important for this space vehicle, along with every space vehicle undergoing re-entry, to predict the behavior for blunt body re-entry problems, as the information is useful to create an op-

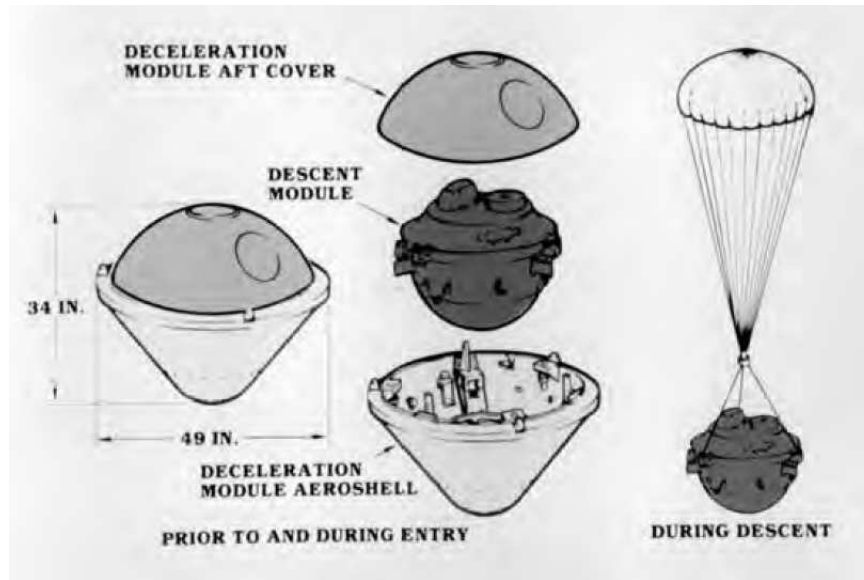


Figure 2: Galileo Probe, which was active in 1997; figure from [2].

timal geometry of a blunt body re-entry vehicle. If the velocity, temperature, and pressure experienced by a re-entry vehicle can be successfully predicted with numerical calculations, then this can ensure the health and safety of astronauts and equipment used to enter the atmosphere.

Most researchers aiming to numerically calculate the shock wave surrounding the blunt body during re-entry have used Euler equations to describe the flow. These equations by definition do not include physical damping, and as a result instabilities with their calculations have arisen near the shock wave. One problem that earlier studies have encountered is the carbuncle phenomenon, which is an instability that does not represent the physical solution to the problem. This carbuncle instability arises when using a specific numerical method, such as Roe's scheme, to solve the Euler equations in time [4]. For sufficiently high Mach numbers, using this type of method will result in major fluctuations, or "wiggles," in the calculated shock wave, which are not physically observed.

To remove the carbuncle instability, researchers often add artificial dissipation to the Euler equations. This method of suppressing the carbuncle instability is a poor method of correcting the instability as it is a post-dictive strategy rather than a predictive strategy. As

a result, using numerical methods that lead to the carbuncle instability will be of no use as a predictive tool for blunt body re-entry. Since the model cannot predict the behavior of a realistic blunt body, it must rather change the solution to match re-entry that is observed. This strategy is also not robust, as the artificial dissipation added can change from each different condition of re-entry used as well as with each computational grid, so the equations cannot be applied to a wide range of re-entry cases.

In this report, a different approach will be taken to numerically predicting the solution to a blunt body re-entry problem. Instead of using the Euler equations, this study will use the compressible Navier-Stokes equations, thus reintroducing the physical damping ignored by the Euler equations. The goal of using the Navier-Stokes equations instead of the Euler equations is to more accurately represent the physical conditions and relationships that exist in nature, and thus get a more accurate solution that does not have the numerical instabilities seen in earlier works. This report will discuss the strategy for using the Navier-Stokes equations, and display the results that accurately depict realistic shock waves from using these equations.

2 Physical Description of Problem

In order to develop a numerical method that successfully predicts the solution to a blunt body re-entry problem, an understanding of the physical problem and the expected solution in nature must be made. One key component of the motion deals with the gas particles flowing around the blunt body as it is in atmospheric re-entry, as the collisions with the molecules and the body tell a lot about the shape and formation of the shock wave surrounding the body. As the blunt body strikes the gas molecules in the atmosphere, the molecules interact with the surface and are ejected off the surface. When the blunt body first enters the atmosphere, the gas has a fairly low density, so the gas molecules that are ejected by the surface of the blunt body do not frequently collide with incoming particles, and the interaction of the

body with the atmosphere can be described by the free molecular flow approximation [3]. However, when the blunt body descends deeper into the atmosphere where the gas becomes more dense, the collisions of ejected molecules and incoming molecules are too frequent to be ignored, and the flow is better modeled as a continuum. These interactions of particles represent the physical damping in the system that is seen in the Navier-Stokes equations. When a blunt body enters the atmosphere, it reaches velocities that are much larger than the speed of sound in the atmosphere, and because of the hypersonic speed a strong bow shock envelops the blunt body, as shown in Figure 3 [3]. The energy contained within a gas

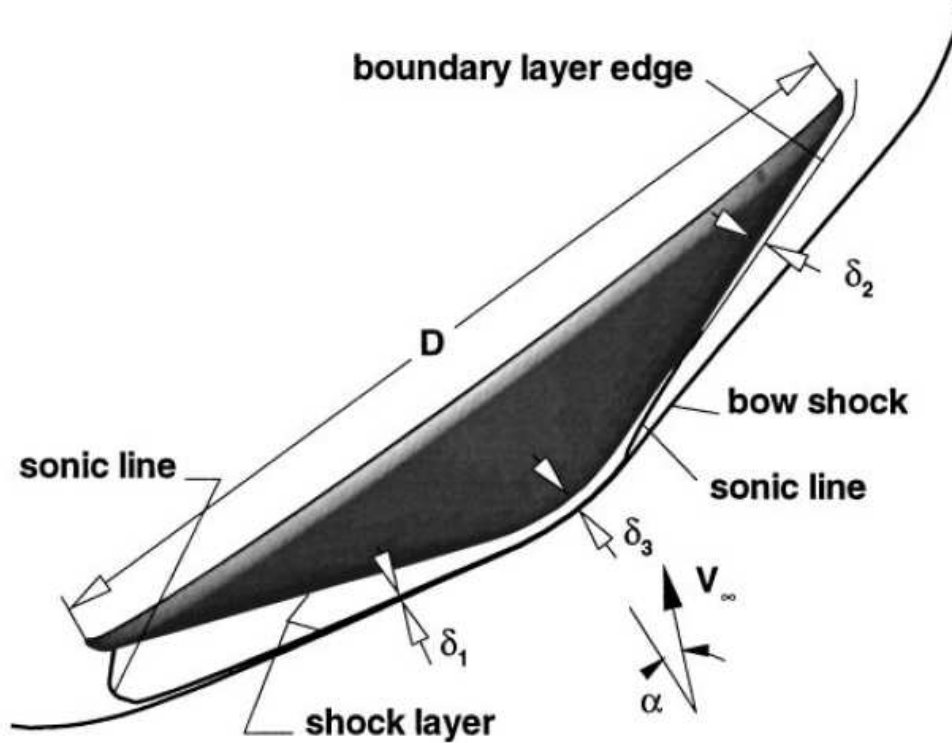


Figure 3: Flowfield over planetary entry vehicle; figure from [3].

molecule that is passing through this bow shock is large. As a result of this high energy and many collisions of particles, a sonic line and shock layer form in this region, along with the creation of chemical reactions between the shock and the body. This region also contains a subsonic region in which the speed of the flow is below the speed of sound. This subsonic region alters for the geometry used for the blunt body, showing that the geometry directly

affects the shock wave produced by supersonic flow [5]. However, the shock wave changes only slightly with a change in body shape, while the shape of the shock wave has a strong dependency on the Mach number of the flow.

3 Prior Research

3.1 Analytical Strategies

Many attempts towards a solution have been attempted in the past decades, each making different assumptions that affect the ease of computation along with the error and convergence of the solution. The oldest known strategy to solve the blunt body problem is through potential flow approximations, which originated in 1947 [6]. This analytical strategy consists of gathering data for subsonic flow around a specific blunt body geometry, then using this air flow and relating it to the actual flow desired, such as the hypersonic flow with a shock wave [7]. This strategy offers an analytical solution, but has shortcomings in that it can only approximate the flow of the air around the blunt body, and cannot predict surface pressures, which is pertinent information for the survival of a re-entry vehicle.

A second analytical strategy is using a Taylor series approximation, created in 1948, in which the detached shock must be known or assumed so that variables such as pressure, density, and velocity can be found using the oblique shock relations [8]. With these variables known, the derivative of these variables can be found by substituting in the equations of motion, which is of the form of a Taylor series. This strategy becomes accurate for axisymmetric flow when using enough terms in the Taylor series so that the solution converges, as shown by Figure 4 [7]. However, this method is not robust for all shock wave forms, as the flow approximation was shown to diverge at the nose of the blunt body for some shock shapes, such as a paraboloidal shock wave [7]. For this case the nose of the axisymmetric flow will never converge to an accurate solution, which is a major problem when computing the flow variables during re-entry. Although the Taylor series approximation is seen to succeed as a

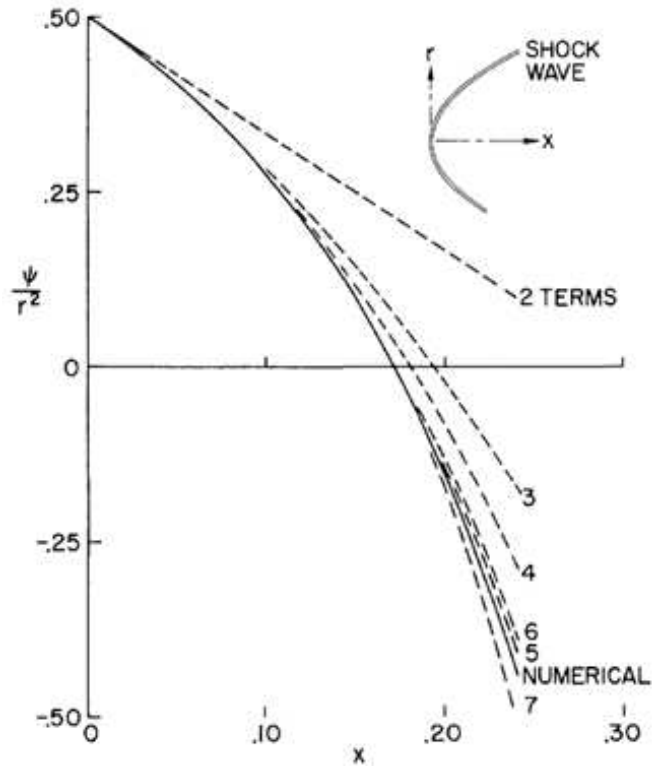


Figure 4: Variation of stream function along axis behind shock wave with a Mach number of $M = 2$ and $\gamma = 7/5$; figure from [7].

qualitative tool for seeing the way that the flow moves, the method is not robust enough to give a consistently accurate solution.

Some approximate methods can be based on simplifying assumptions that represent the more complex mathematical model in order to be able to compute the solution [5]. One assumption is to approximate the flow as incompressible, which originated in 1953 [9]. This is a valid assumption for blunt bodies moving at very high supersonic speeds. At these speeds, where the Mach number is large, the density only varies slightly between the shock wave and surface of the body, leading to the assumption of an incompressible flow. After making the assumption of an incompressible solution, a numerical solution can be calculated for flow in a stream of near infinite Mach number. This gives fairly accurate results and remains stable with a reasonable step size, but has error due to the lack of incorporation of compressibility [7]. A different analytical strategy with a different assumption uses the

Newtonian approximation, which originated in 1948 [10]. The Newtonian theory states that fluid particles lose their normal component of momentum during collisions with the surface of the blunt body, so this strategy numerically computes the solution of the flow under this assumption [7]. This computation converges very slowly for axisymmetric flow, and is inadequate for computing the pressure of the air in the flow. Although these strategies are sufficient to present a rough estimate of the solution and to form premises about the flow, a better computational strategy is necessary in order to find a sufficiently accurate and robust solution to the supersonic flow.

A very early attempt at a shock-capturing method was completed by Evans and Harlow [11]. In their computation, the gas was represented by Lagrangian mass points that were numerically computed with the Euler equations, and the flow region adjacent to the front of the blunt body cylinder was studied. This solution provided a good qualitative presentation of the formation of a shock wave, but many inaccuracies arose from the computation. The flow near the cylinder face was poorly represented by the computation, and as a result had to be drawn in approximately. The coarse mesh created inaccuracies with some physically observed instances of a shock formation, as the detached shock was significantly away from the observed location. Although this research provided the grounds for a new strategy for capturing a shock wave, it also introduced more inaccuracies and problems with its solution.

Another strategy towards calculating the flow of a shock wave around a blunt body was through a shock-fitting technique, which was attempted by Moretti and Abbott [12]. This technique consisted of prescribing the body geometry to control the computation, and assuming a shock shape in order to fit to the body in computation [12]. The points along the shock and the body were computed differently than the points along the interior of the flow region, and the solution was calculated in time from unsteady flow to settle to steady flow [12]. Although this provided seemingly more accurate results than that of the initial shock-capturing techniques, some drawbacks still existed with the solution. One weakness of the shock-fitting technique is that the shock shape was assumed for the computation, so

if the shape is not known prior to calculation then the technique will be hard to implement. Another weakness is that the shock wave was assumed to act as a discontinuity for ease of computation, which could render results inaccurate if the shock wave location was shifted in any way, and does not relate the flow in front and behind the shock [12].

The MacCormack method marked a new type of solution that would provide a different approach at solving the blunt body re-entry problem [13]. This method focused on using the Navier-Stokes equations instead of the typical Euler equations, and performing viscous calculations of the blunt body flow [13]. Although this method closely resembles the strategy used in this research, problems still arose from the calculations. One problem with this solution is that some points were skipped over for ease of computation, and the mesh was relatively coarse [13]. As a result, the solution could be inaccurate and instabilities could appear if a finer mesh is used. Although this strategy has been famously applied to this problem, various complexities with the method rendered it not adequate as a universal solution strategy.

3.2 Instabilities

When calculating the shock wave in supersonic flow, earlier research has uncovered a variety of instabilities [7]. One of the instabilities arises from the initial value problem used when calculating the shock wave. One numerical method used to calculate the shock wave requires the information in front of the shock in order to calculate the rest of the flow. If the hydrodynamic properties are known at the shock, such as the pressure, density, and entropy, then a system of hydrodynamical equations can be solved for the rest of the flow, including the shock [8]. This treats the problem as an initial value problem; if the initial values before the shock occurs are known, then the flow behind the shock can be solved for and thus the solution to the flow can be found. However, this method of calculating the shock has been found to be unstable based on the initial conditions given. This means that for only a small error in the initial value, the error grows rapidly throughout the mesh as the solution is

calculated in geometric progression. This is shown by Figure 5 [7]. If many steps are taken

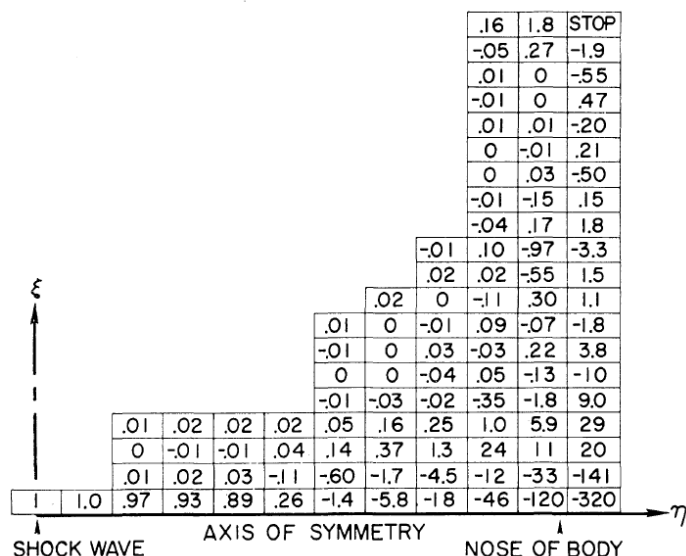


Figure 5: Variation of stream function along axis behind shock wave with a Mach number of $M = 2$ and $\gamma = 7/5$; figure from [7].

between the shock and the body, or a fine mesh size is used, then this instability can destroy the accuracy of the entire solution.

The most prominent instability found when calculating the flow over a supersonic blunt body is known as the carbuncle phenomenon, and is found when using the Euler equations to calculate the numerical solution with some well known methods such as Roe’s method [14]. This instability is known to be purely a numerical instability, as using different numerical methods results in the appearance or disappearance of the carbuncle instability. This is shown in Figure 6, as one numerical method (Roe’s scheme) gives rise to the carbuncle instability while the other creates a stable and physically accurate solution [4]. One observation that shows how the carbuncle is numerically based is the reliance on the grid with the solution. The carbuncle instability is more likely to appear when the shock wave is located on a grid line, as well as when the grid cells are very elongated along a direction normal to the shock [4]. When the shock is being captured by the flow field, the main cause of the carbuncle instability is the shock strength. Consequently, when a shock-fitting technique is

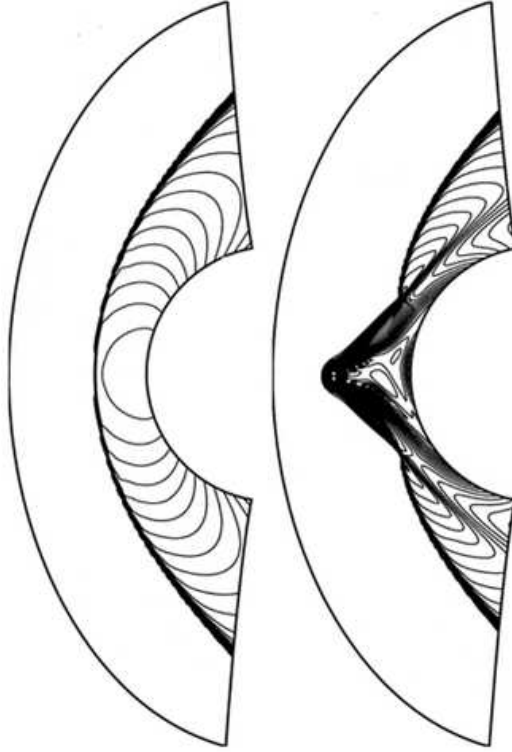


Figure 6: Physically acceptable result of temperature in shock (left) compared with result with carbuncle instability when using Roe's scheme; figure from [4].

used, where the shape of the shock can be assumed prior to calculation, the instability disappears. However, when a shock-capturing technique is used the carbuncle can appear when higher order methods are in use [14]. The carbuncle's appearance has also been attributed to the imbalance of dissipation throughout the flow of the solution [15].

Some methods are successful in consistently keeping the carbuncle phenomenon from appearing, most involving the addition of artificial damping. These obtain an accurate solution when using the Euler equations to numerically solve for the flow, but cost the solution reliability since they include effects not seen in nature. An example of one of these sorts of methods is the HLLE method, which adds strong artificial damping to the system [4]. Although this method will obtain a correct solution when using the Euler equations, the boundary layer will be significantly broadened if using the Navier-Stokes equations to solve for the supersonic flow. Even if the solution was accurate to the physical model, the

computation added artificial damping that is not seen in nature, and there is no physical justification for adding artificial damping [14]. Thus, artificial damping is not a robust enough fix to cover variations of the same shock problem.

4 Navier-Stokes Equations

The compressible Navier-Stokes equations for an isotropic Newtonian fluid were used in order to numerically predict the solution of the blunt body re-entry problem. The set of equations, using 19 equations to solve for 19 unknowns, are shown below:

$$\frac{d\rho}{dt} = -\rho\nabla \cdot \mathbf{v} \quad (1)$$

$$\rho \frac{d\mathbf{v}}{dt} = -\nabla P + \nabla \cdot \boldsymbol{\tau} \quad (2)$$

$$\rho \frac{de}{dt} = -\nabla \cdot \mathbf{q} - P\nabla \cdot \mathbf{v} + \boldsymbol{\tau} : \nabla \mathbf{v} \quad (3)$$

$$\boldsymbol{\tau} = \mu(\nabla \mathbf{v} + \nabla \mathbf{v}^T) - \frac{2}{3}\mu(\nabla \cdot \mathbf{v})\mathbf{I} \quad (4)$$

$$\mathbf{q} = -k\nabla T \quad (5)$$

$$P = \rho RT \quad (6)$$

$$e = c_v T \quad (7)$$

In these equations, the following variables were used: ρ is the density in kg/m³ (scalar), t is the time in s (scalar), \mathbf{v} is the velocity in m/s (vector), P is the pressure in N/m² (scalar), $\boldsymbol{\tau}$ is the viscous stress in N/m² (symmetric tensor), e is the specific internal energy in J/kg (scalar), \mathbf{q} is the heat flux vector in W/m² (vector), μ is the first coefficient of viscosity in Ns/m² (scalar), T is the temperature in K (scalar), \mathbf{I} is the identity matrix, k is the thermal conductivity in W/m/K (scalar), R is the universal gas constant for air in J/(kg K) (scalar), and c_v is the specific heat at constant volume in J/(kg K) (scalar). Equation (1) describes the conservation of mass, Equation (2) represents Newton's second law, Equation (3) represents the first law of thermodynamics, Equation (4) gives the stress-strain rate relationship for

isotropic Newtonian fluids which satisfy Stokes' assumption, and Equation (5) displays the definition of heat flux [16]. Equations (6) and (7) are the thermal and caloric equations of state, respectively, for a calorically perfect ideal gas. These equations were discretized and solved by advancing discretely in time to find the steady-state solution to the blunt body re-entry problem.

5 Numerical Approach

5.1 Boundary Conditions

To calculate the flow field in blunt body re-entry, a geometry was created with certain boundary conditions specified. Figure 7 displays the geometry of the mesh used in the numerical computation, with boundary conditions specified. The inflow boundary had Dirichlet

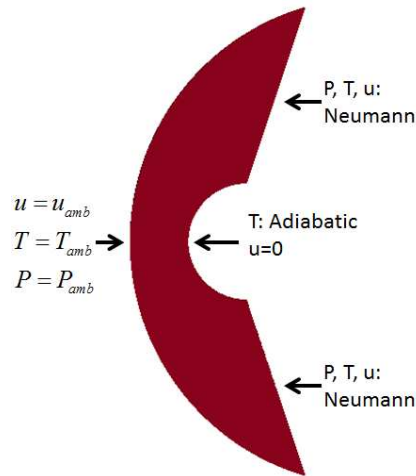


Figure 7: Geometry of mesh used for numerical solution, with boundary conditions specified at each face.

boundary conditions for the pressure, temperature, and velocity, where each was set to the respective ambient value. The outflow boundaries had Neumann boundary conditions with zero gradient, as the air flow was assumed to retain the conditions past the mesh as the air flows past the blunt body. The inner cylinder, which represents the blunt body, was set to a

no-slip condition, as the velocity was fixed at zero. The inner cylinder also had an adiabatic condition. The initial conditions were also set in this mesh, as the field of data points in the mesh were initially set to the ambient values of pressure, temperature, and velocity, which would assume that the blunt body was instantaneously placed in the supersonic flow. Although this initial condition is not physically plausible, this condition helped to achieve the steady state solution at a faster rate while still using the same computational strategy. Since the mesh only covers the domain in front of the blunt body, only the shock wave and boundary layer were computed, and the wake created from re-entry was omitted.

5.2 One-Dimensional Solution

To estimate the thickness of the shock that would be seen in the solution, a one dimensional shock problem with the same conditions was calculated in `Mathematica`. The equations used are shown below:

$$\rho u = \rho_o u_o \quad (8)$$

$$\tau_{xx} = \tau_{xxo} + \rho u^2 + P - \rho_o u_o^2 - P_o \quad (9)$$

$$q_x - q_{xo} + \tau_{xxo} u_o - \tau_{xx} u = \rho_o u_o \left(e_o + \frac{u_o^2}{2} \right) + P_o u_o - \rho u \left(e + \frac{u^2}{2} \right) - P u \quad (10)$$

$$P = \rho R T \quad (11)$$

$$e = c_v T \quad (12)$$

$$q_x = -k \frac{dT}{dx} \quad (13)$$

$$\tau_{xx} = \frac{4}{3} \mu \frac{du}{dx} \quad (14)$$

From this model, the shock thickness could be estimated by calculating a one-dimensional shock with the same parameters as the two-dimensional blunt body problem, which were specified to be:

- $c_v = 717.625 \text{ J}/(\text{kg K})$

- $R = 287 \text{ J}/(\text{kg K})$
- $\mu_o = 1.488 \times 10^{-5} \text{ kg}/(\text{m s})$
- $k_o = 0.0263 \text{ W} / (\text{m K})$
- $\mu = 1.488 \times 10^{-5} \text{ kg}/(\text{m s})$
- $M = 3.5$
- $T_{amb} = 300 \text{ K}$
- $P_{amb} = 100 \text{ Pa}$
- $\gamma = \frac{7}{5}$
- $Pr = 0.72$

The resulting shock thickness could be assumed to be the shock thickness in the blunt body re-entry problem. Figure 8 shows a plot of temperature with respect to distance in the one-dimensional shock problem. From this plot, the shock thickness could be estimated to be of the order of 10^{-4} m . This approximation led to the choice of spatial resolution and size of the blunt body to use for the shock calculation.

5.3 Discretization and Numerical Schemes

In order to capture the shock in the calculation, ten or more data points were needed within the viscous shock in order to fully capture the shock. To do this, the mesh size used was $1 \times 10^{-6} \text{ m}$, which was a conservatively fine mesh in order to capture the shock. Equation (15) shows how the time step used was approximated:

$$\Delta t \sim \frac{\Delta x^2}{\nu}, \quad (15)$$

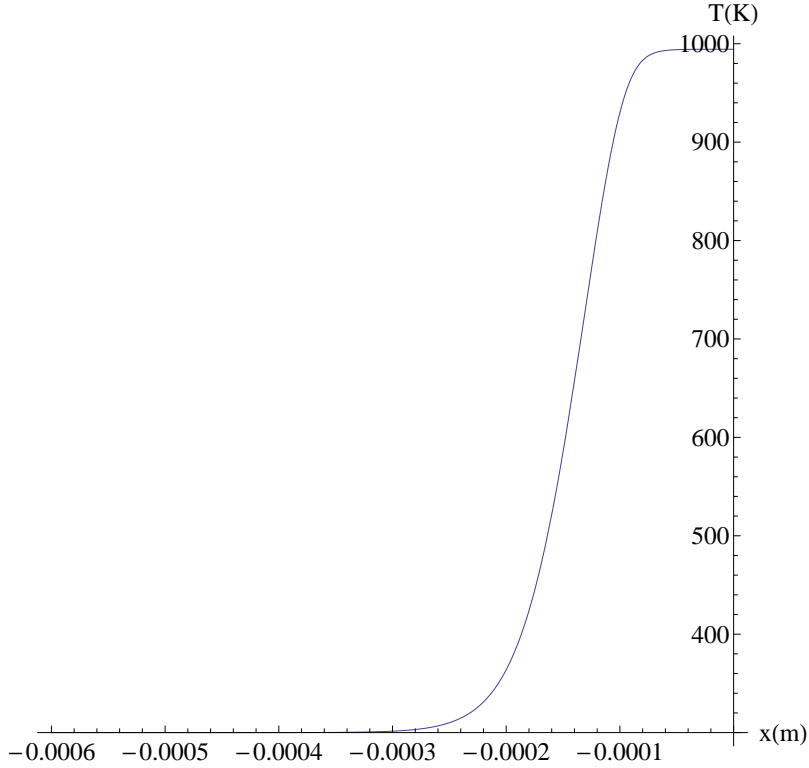


Figure 8: Temperature with respect to distance for one-dimensional shock problem.

where ν is the kinematic viscosity $\nu = \mu/\rho$ of the fluid, which is known to be of the order of $\nu \sim 10^{-5} \text{ m}^2/\text{s}$. The time step used was $\Delta t = 1 \times 10^{-11} \text{ s}$. In order to compute at an efficient rate, the cylinder must be small enough so that minimum data points are used in the computation. With this in mind, the cylinder was chosen to have a radius of $r = 1 \times 10^{-4} \text{ m}$. This allowed there to be 100 points in one direction to cover the length of the shock. Figure 9 shows the geometry with the grids exposed. When calculating the solution to the Navier-Stokes equations to find a solution to the blunt body re-entry problem, a first order upwind numerical scheme was used to numerically solve the solution. The end time for the solution was $t_{final} = 1 \times 10^{-6} \text{ s}$, in which the solution was predicted to reach steady state.

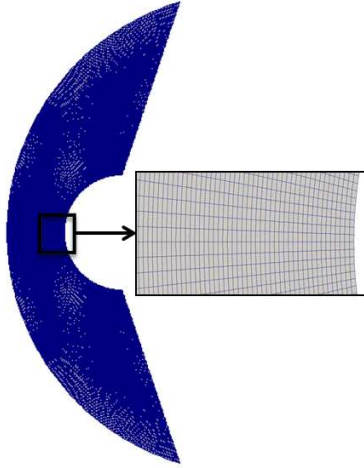


Figure 9: Grids used in geometry, with a zoomed in section near the blunt body boundary.

6 Results

6.1 Re-entry Conditions

The re-entry parameters from the one-dimensional solution were also applied to the two-dimensional solution. These parameter values model conditions that might be expected in the upper atmosphere. The ambient pressure was kept at a relatively low value that more resembled the ambient pressure in the stratosphere, known to have an ambient pressure about 1000 times less than that at sea level which is 101325 Pa [17]. This low pressure was used so that the thickness of the shock would be larger, which is beneficial for the numerical solution to resolve the shock. Equation (16) shows how the derived parameter of blunt body velocity was found with these parameter values,

$$u_{amb} = M\sqrt{\gamma RT}, \quad (16)$$

in which the velocity was found to be $u_{amb} = 1215.16$ m/s.

6.2 Plots of results

The results for velocity of magnitude $|\mathbf{v}| = \sqrt{u^2 + v^2}$ and pressure at steady state are shown in Figure 10. The velocity magnitude field has a resolved shock around the blunt body, and the velocity diminishes to zero around the boundary of the inner cylinder. The maximum pressure occurs at the front of the blunt body cylinder, and dissipates as the flow leaves the mesh. The results for temperature and density at steady state are shown in Figure 11.

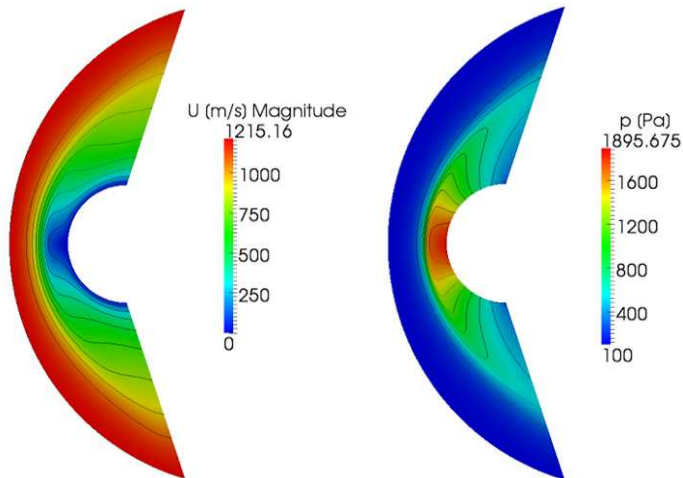


Figure 10: Velocity (left) and pressure (right) surrounding blunt body at $t = 1 \times 10^{-6}$ s.

The maximum temperature and density occurs at the front of the blunt body cylinder, and dissipates as the flow leaves the mesh.

7 Conclusion

The results show that using the Navier-Stokes equations instead of the commonly used Euler equations to calculate blunt body re-entry cures the carbuncle problem. The figures of pressure, velocity, temperature, and density all compare accurately to what is seen in nature, displaying how instabilities were removed by calculating the solution with viscosity. A fine space and time grid were required to compute the solution, as the grid points needed to be fine enough to resolve the flow physics. If this criteria was achieved, then the carbuncle

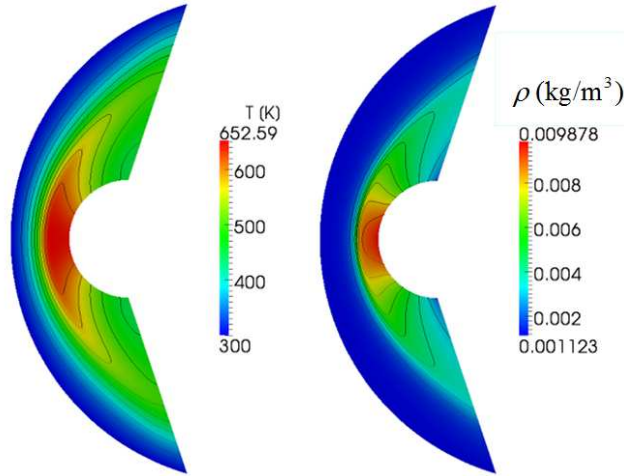


Figure 11: Temperature (left) and density (right) surrounding blunt body at $t = 1 \times 10^{-6}$ s.

instability, or “wiggles” seen in the shock wave, were successfully removed from the numerical calculation.

8 Future Work

Future work with this study consists of many different parametric studies using this computation strategy. Different parameters will be varied such as Mach number and ambient pressure to see if the computation strategy will remain robust and accurate for calculating blunt body re-entry. The geometry of the blunt body and mesh surrounding it could also be changed, along with adding high temperature physics and seeing its effects on the solution. While changing all of these different variables, the different solutions could be investigated to see if instabilities other than the carbuncle phenomenon arise from using the Navier-Stokes equations instead of the Euler equations. Other modes of oscillations could be possible when using the Navier-Stokes equations, so the numerical error can be further studied to make sure that the results are repeatable and robust. From this research, a clear strategy for computing the blunt body re-entry problem can be formed and thus forming a repeatable method for calculation.

9 References

- [1] Van Dyke, M., 1982, *An Album of Fluid Motion*, Parabolic Press, Stanford, California.
- [2] Metltzer, M., 2007, *Mission to Jupiter: A History of the Galileo Project*, NASA, Washington, DC.
- [3] Gnoffo, P.A., 1999, “Planetary-Entry Gas Dynamics”, *Annual Review of Fluid Mechanics*, 31: 459-494.
- [4] Robinet, J., Gressier, J., Casalis, G., and Moschetta, J., 2000, “Shock Wave Instability and the Carbuncle Phenomenon: Same Intrinsic Origin?” *Journal of Fluid Mechanics*, 417: 237-263.
- [5] Rusanov, V.V., 1976, “A Blunt Body in a Supersonic Stream,” *Annual Review of Fluid Mechanics*, 8: 377-404.
- [6] Laitone, E. V., and Pardee, O. O’M., 1947, “Location of Detached Shock Wave in Front of a Body Moving at Supersonic Speeds,” National Advisory Committee for Aeronautics, NACA RM No. A7B10.
- [7] Van Dyke, M. D., 1958, “The Supersonic Blunt-Body Problem—Review and Extension,” *Journal of the Aerospace Sciences*, 25(8): 485-496.
- [8] Lin, C.C. and Rubinov, S.I., 1948, “On the Flow Behind Curved Shocks,” *Journal of Mathematics and Physics*, 27(2): 289-313.
- [9] Hida, K., 1953, “An Approximate Study on the Detached Shock Wave in Front of a Circular Cylinder and a Sphere,” *Journal of the Physical Society of Japan*, 8(6): 740-745.
- [10] Ivey, H. R., Klunker, E. B., and Bowen, E. N., 1948, “A Method for Determining the Aerodynamic Characteristics of Two- and Three-Dimensional Shapes at Hypersonic Speeds,” National Advisory Committee for Aeronautics, NACA TN No. 1613.
- [11] Evans, M.W. and Harlow, F.H., 1958, “Calculation of Supersonic Flow Past an Axially Symmetric Cylinder,” *Journal of the Aeronautical Sciences*, 25(4): 269-270.
- [12] Moretti, G. and Abbett, M., 1966, “A Time-Dependent Computational Method for

- Blunt Body Flows,” *AIAA Journal*, 4(12): 2136-2141.
- [13] MacCormack, R.W., 1982, “A Numerical Method for Solving the Equations of Compressible Viscous-Flow,” *AIAA Journal*, 20(9): 1275-1281.
- [14] Quirk, J.J., 1994, “A Contribution to the Great Riemann Solver Debate,” *International Journal for Numerical Methods in Fluids*, 18(6): 555-574.
- [15] MacCormack, R.W., 2013, “Carbuncle Computational Fluid Dynamics Problem for Blunt-Body Flows,” *Journal of Aerospace Information Systems*, 10(5): 229-239.
- [16] Powers, J. M., 2012, *Lecture Notes on Gas Dynamics*, Department of Aerospace and Mechanical Engineering, University of Notre Dame, Notre Dame, Indiana 46556, 20-31. <http://www3.nd.edu/~powers/ame.30332/notes.pdf>
- [17] Kuethe, A. M. and Chow, C.Y., 1998, *Foundations of Aerodynamics*, John Wiley, New York.